

# Calibrated and uncertain? Evaluating uncertainty estimates in binary classification models

**Aurora Grefsrud**  
**Trygve Buanes**

*Department of Computer science, Electrical engineering and Mathematical sciences  
 Western Norway University of Applied Sciences  
 5063 Bergen, Norway*

AGRE@HVL.NO  
 TRBU@HVL.NO

**Nello Blaser**

*Department of Informatics  
 University of Bergen  
 5020 Bergen, Norway*

NELLO.BLASER@UIB.NO

## Abstract

Rigorous statistical methods, including parameter estimation with accompanying uncertainties, underpin the validity of scientific discovery, especially in the natural sciences. With increasingly complex data models such as deep learning techniques, uncertainty quantification has become exceedingly difficult and a plethora of techniques have been proposed. In this case study, we use the unifying framework of approximate Bayesian inference combined with empirical tests on carefully created synthetic classification datasets to investigate qualitative properties of six different probabilistic machine learning algorithms for class probability and uncertainty estimation: (i) a neural network ensemble, (ii) neural network ensemble with conflictual loss, (iii) evidential deep learning, (iv) a single neural network with Monte Carlo Dropout, (v) Gaussian process classification and (vi) a Dirichlet process mixture model. We check if the algorithms produce uncertainty estimates which reflect commonly desired properties, such as being well calibrated and exhibiting an increase in uncertainty for out-of-distribution data points. Our results indicate that all algorithms are well calibrated, but none of the deep learning based algorithms provide uncertainties that consistently reflect lack of experimental evidence for out-of-distribution data points. We hope our study may serve as a clarifying example for researchers developing new methods of uncertainty estimation for scientific data-driven modeling.

## 1 Introduction

Scientists deciding whether to use deep learning or other advanced statistical methods in their data analysis need to understand how reliable their results are. In classical statistical methods traditionally used in natural science research, estimated values come with uncertainties, which serve exactly this purpose. Scientists expect high uncertainties to be an indicator that they should not trust the results much, and that they may need to collect more data or re-evaluate their experiment before making any decisions or scientific claims. When we instead turn to more complex statistical methods, where the inner workings of the algorithms become unclear to scientists (making them essentially black box models), estimating uncertainty becomes both more difficult and more important.

In this study we will focus on classification problems. These are tasks where data is sorted into predefined categories based on their features, which are often assumed to be

continuous variables. Examples in the natural sciences include determining the gender of fish based on parameters such as length and weight, categorizing patients into positive or negative for a disease based on medical test results or classifying jets produced by the decay of unstable particles in high energy particle physics collision experiments based on jet constituent features. The classifier algorithms we investigate in this study estimate the probability of a new data point belonging to each of the possible classes, as well as the uncertainty of this probability.

Bayesian inference methods for classification ranging from simple parametric logistic regression to infinite dimensional nonparametric models result in probability distributions over class probabilities. Approximations of the mean of these distributions are often used as class probability estimates and the variance (or standard deviation) provide a measure of uncertainty over the space of possible solutions. Deep learning methods using stochastic gradient descent and early stopping however, typically only results in point estimates of the mode via maximum a posteriori optimization (Mandt et al., 2017; Duvenaud et al., 2016). Such maximization methods, similarly to maximum likelihood estimation, do not assess the variance of possible solutions, leading to lack of information about the uncertainty of the final posterior distribution.

Various enhanced neural network classifiers aim to mitigate this issue by providing uncertainty estimates (Hüllermeier and Waegeman, 2021; Abdar et al., 2021). One of the main selling points of these algorithms is that they will warn us about anomalous, also known as out-of-distribution (OOD), data because we intuitively assume that uncertainties will be high and, in the case of binary classification, probability estimates will be close to 0.5 for this kind of data. However, uncertainty estimates from ensembling, Monte Carlo Dropout and other neural network based algorithms have been shown to give arbitrarily low uncertainty estimates for OOD data (Liu et al., 2021).

The fidelity of the in-distribution estimated class probabilities themselves has also been a topic of much debate. A well calibrated classifier outputs class probability estimates that on average match the empirical class frequency distribution. There is conflicting empirical evidence in the literature on the calibration properties of neural network classifiers. Some studies show that point estimates are not calibrated, raising concerns about their reliability (Guo et al., 2017). Other studies show that neural networks actually are well calibrated (Niculescu-Mizil and Caruana, 2005; Minderer et al., 2021). The field of uncertainty quantification in machine learning is unfortunately fraught with inconsistency, lack of theoretical justification and widespread disagreement on fundamental terms such as probability, uncertainty, and calibration, further exacerbating confusion (Trivedi and Nord, 2025; Perez-Lebel et al., 2023).

The aim of this study is to contribute to a clearer understanding in the field of uncertainty quantification and probabilistic machine learning with a focus on binary classification. We do this by clarifying the concepts of class probability, calibration, uncertainty estimates and out-of-distribution predictions, using the theoretical framework of probability calculus and approximate Bayesian inference. In addition, we have performed a case study where we use these theoretical insights to evaluate qualitative properties of six different probabilistic learning algorithms for class probability and uncertainty estimation: (i) a neural network ensemble (MacKay, 1995), (ii) neural network ensemble with conflictual loss (Fellaji et al., 2024), (iii) evidential deep learning (Sensoy et al., 2018), (iv) neural network with Monte

Carlo Dropout (Gal and Ghahramani, 2016), (v) Gaussian process classification (Rasmussen and Williams, 2006) and (vi) a Dirichlet Process Mixture Model (Li et al., 2019). The study investigates the estimates produced by the different algorithms using synthetic data with a clearly defined generating function with smoothly varying densities, inspired by common assumptions made in natural science experiments. Specifically, we address the following three research questions in the case of our data:

- Q1: Are the estimated probabilities calibrated, that is, are they unbiased and converge towards the long-run frequency distribution?
- Q2: Do the uncertainty estimates go down, on average, with increasing amounts of training data?
- Q3: Does uncertainty increase for out-of-distribution data, that is, does it increase as we move further away from the bulk of the training data?

The research questions and relevant terminology are explained further in sections 2 and 4. The algorithms tested are described in Appendix A. We hope that our study can serve as an intuitive and easy to implement example of employing toy studies for researchers looking into developing new uncertainty quantification methods using theoretically founded methodology.

## 2 Theory

In this section we will describe the theoretical concepts relevant to the case study. We assume the reader is familiar with basic probability theory, Bayesian, and frequentist statistics, but recap the most important aspects before explaining the concept of calibration and out-of-distribution overconfidence. Further we introduce the mean and standard deviation of the posterior distribution as our class probability and uncertainty estimates and explain how these can be calculated.

### 2.1 The need for a theory of deep learning

In the age of big-data driven modeling and decision making, where the complexity of data and statistical models continue to grow as computing power and storage capacity increases, great opportunities but also critical challenges face scientists wanting to take advantage of this new wealth of information (Fan et al., 2014). In the natural sciences, perhaps the most pressing of these issues is the need for robust and theoretically well founded statistical methods (Matureo et al., 2025). This is important because basic research in the natural sciences is especially dependent on public trust for its funding and credibility, and publishing wrong results based on faulty assumptions about the statistical methods used can potentially be devastating.

Machine learning techniques such as deep learning, a family of algorithms using artificial neural networks to learn from data and make predictions on unseen data, have proved to be extremely effective tools for problems involving big complex datasets. However, there has traditionally been a lack of interest in establishing mathematical theoretical foundations in the successfully empirically-driven field of deep learning (Breiman, 2001). Despite this,

as deep learning has shown itself to be exceptionally effective at solving real-life problems, significant effort has been put into theory development as described in an overview by He and Tao (2020), who classifies attempts at theory development into six different categories. Their category “Stochastic differential equations for modeling stochastic gradient descent and its variants” encompasses the Bayesian approach to the problem, and this is also the approach we use.

## 2.2 Probability theory

We consider the following very general model of our data. A dataset with  $N$  independent, identically distributed samples  $\mathcal{D}_N = \{d_1, d_2, d_3, \dots, d_N\}$ , with  $d_i = (\mathbf{c}_i, \mathbf{x}_i)$  is created by sampling from the underlying joint probability distribution  $p(\mathbf{c}, \mathbf{x})$ . We let the one-hot vector  $\mathbf{c}_i$  indicate the binary<sup>1</sup> class label, a nominal variable, which can take on the values  $[1, 0]$  (class 1) or  $[0, 1]$  (class 2). We consider the input features  $\mathbf{x}_i$  to be continuous  $n$ -dimensional vectors  $\mathbf{x}_i = [x_i^1, x_i^2, \dots, x_i^n] \in \mathbb{R}^n$ . The aim of the classification problem is to estimate the discrete conditional class probability distribution of a new data point  $d_{N+1}$ ,  $\mathbf{P}(\mathbf{c}_{N+1}|\mathbf{x}_{N+1}) = [P(c_{N+1}^1 = 1|\mathbf{x}_{N+1}), P(c_{N+1}^2 = 1|\mathbf{x}_{N+1})]$ , where  $P(c^1 = 1|\mathbf{x}) + P(c^2 = 1|\mathbf{x}) = 1$ .

The conditional class probability distribution may be rewritten as a categorical distribution parametrized by  $\nu(\mathbf{x})$  as  $P(\mathbf{c}|\nu(\mathbf{x})) = \nu(\mathbf{x})^{c^1} \cdot (1 - \nu(\mathbf{x}))^{c^2}$ . We can express  $\nu$  in terms of the conditional densities  $P(\mathbf{x}|\mathbf{c})$  using Bayes formula

$$\nu(\mathbf{x}) = P(c^1 = 1|\mathbf{x}) = \frac{p(\mathbf{x}|c^1 = 1)p(c^1 = 1)}{p(\mathbf{x}|c^1 = 1)p(c^1 = 1) + p(\mathbf{x}|c^2 = 1)p(c^2 = 1)}. \quad (1)$$

If there is overlap in the conditional densities, classification is not deterministic.

## 2.3 Calibration properties

The frequency interpretation of probability becomes immediately clear if we consider a dataset sampled from  $p(\mathbf{c}, \mathbf{x})$  with  $N$  samples. The limit of the sample frequencies of each class (the empirical frequency distribution) in any closed set  $A_\epsilon \in X^n$  with volume  $\epsilon$  for  $\epsilon \rightarrow 0$  and  $N \rightarrow \infty$  are equal to the class probabilities  $\mathbf{P}(\mathbf{c}|\mathbf{x})$ . For this reason we will refer to  $\mathbf{P}(\mathbf{c}|\mathbf{x})$  as the long-run frequency distribution (LRFD), although this quantity is often referred to as the true underlying probabilities, true probabilities, real probabilities and the true posterior distribution (Perez-Lebel et al., 2023). The empirical frequency distribution, which is also the maximum likelihood estimate for the Bernoulli distribution, is unbiased as its expectation value for any size dataset equals  $\nu(\mathbf{x})$ . The calibration literature is focused on evaluating if a classifier’s output matches the empirical frequency distribution of the test set (Nixon et al., 2019; Rubin, 1984). This estimator however, poses a problem when we want to look into the tails of the distribution, as explained in the following.

If we do not have any prior information about the distribution in question we need to choose an uninformative prior which assigns equal probabilities to both classes to do Bayesian inference (Zhu and Lu, 2004; Jaynes, 2003; Bernardo and Smith, 2000). For a

---

1. Extension to more than two classes is fairly trivial at this point, but turns out to not be as simple in practice, so we will just consider the binary case.

Bernoulli distribution with probability of success  $\nu$  (observations of class 1), such as in our binary classification task, the conjugate prior is the Beta distribution with density

$$\text{Beta}(\alpha, \gamma) = \frac{\Gamma(\alpha + \gamma)}{\Gamma(\alpha)\Gamma(\gamma)} \nu^{\alpha-1} (1 - \nu)^{\gamma-1},$$

where  $\Gamma$  is the Gamma function and  $\alpha, \gamma$  are its parameters. The resulting posterior for an experiment resulting in  $N$  trials and  $S$  observations of class 1 is also a Beta distribution with density

$$p(\nu|N, S) \propto \nu^{\alpha+S-1} (1 - \nu)^{\gamma+N-S-1},$$

and therefore

$$\mathbb{E}[P(c^1 = 1|\mathbf{x})] = \mathbb{E}[\nu] = \int_0^1 p(\nu|N, S) \nu d\nu = \frac{S + \alpha}{N + \alpha + \gamma}.$$

This estimator is consistent as  $\lim_{N, S \rightarrow \infty} \mathbb{E}(\nu) = \nu$ , but not necessarily unbiased.

To get the desired  $\mathbb{E}(\nu) = 0.5$  for  $N = S = 0$  required by an uninformative prior, we have to set  $\alpha = \gamma = c$ . This gives us a mean and variance of

$$\mathbb{E}[P(c^1 = 1|\mathbf{x})] = \mathbb{E}[\nu] = \frac{S + c}{N + 2c}, \quad (2)$$

$$\text{Var}[P(c^1 = 1|\mathbf{x})] = \text{Var}[\nu] = \frac{(N - S + c)(S + c)}{(N + 2c + 1)(N + 2c)^2} = \frac{\mathbb{E}[\nu](1 - \mathbb{E}[\nu])}{(N + 2c + 1)}. \quad (3)$$

As explained by Zhu and Lu (2004), the choice of  $c$  determines how strong the influence of the prior is on the posterior. Letting  $c$  go towards 0 leads to the unbiased maximum likelihood estimator  $\lim_{c \rightarrow 0} \mathbb{E}(\nu) = \lim_{c \rightarrow 0} (S + c)/(N + 2c) = S/N$ , and also the largest possible variance. This prior is essentially two point masses of probability at 1 and 0. If we make one observation of class 1,  $S = N = 1$ , and insert this data into the formula for the posterior, it will (when we approach the limit) shift the expected class frequency completely towards that outcome, which implies a high confidence for the next prediction, contrary to our intuition for an experiment with only one datapoint. Setting  $c$  instead to 1 specifies a flat prior over  $\nu$  and gives us the Bayes-Laplace estimator  $\mathbb{E}(\nu) = (1 + S)/(2 + N)$ , the posterior mean of the probability of class 1 for a new data point will be  $\frac{2}{3}$ , a much less extreme departure from the  $S = N = 0$  case. If we want to reduce overconfident estimates for class probability when there is little data, we should choose a prior with stronger bias towards 0.5. In this case, our estimates will not be well calibrated (unbiased) for few datapoints, but the model will be less prone to high-confidence error. It is therefore necessary to separate the discussion of in-distribution (locally high training statistics) calibration where the bias from the prior is insignificant from the discussion of out-of-distribution (locally low training statistics) predictions where a bias is desirable.

## 2.4 Approximate Bayesian inference

If we consider  $\nu$  to be an analytical function  $\nu(\mathbf{x})$  of  $\mathbf{x}$ , we can integrate over every possible function  $\nu(\mathbf{x})$  to find the mean of the posterior

$$\mathbb{E}[\nu(\mathbf{x})] = \int \nu(\mathbf{x}) p(\nu(\mathbf{x}) | \mathcal{D}_N) d\nu(\mathbf{x}) = \int \nu(\mathbf{x}) \frac{p(\mathcal{D}_N | \nu(\mathbf{x})) p(\nu(\mathbf{x}))}{p(\mathcal{D}_N)} d\nu(\mathbf{x}),$$

$$\text{where } p(\mathcal{D}_N | \nu(\mathbf{x})) = \prod_{i=1}^N \nu(\mathbf{x}_i)^{c_i^1} \cdot \prod_{i=1}^N (1 - \nu(\mathbf{x}_i))^{c_i^2}.$$

At this point one must make some assumptions about what every possible  $\nu$  means, which prior probabilities to assign to  $\nu(\mathbf{x})$ , and if necessary how to approximate this integral. The most common approach is to use parametric methods, which reduce the function-space by making it finite dimensional. On the other hand, nonparametric Bayesian inference methods allow us to keep the integral infinite dimensional. These latter methods are the “gold standard” for uncertainty estimation, as they are theoretically well founded and have properties that tend to align with how we wish uncertainty to behave, such as increased uncertainty in low density regions of data space. Examples of such methods are Gaussian Processes and Dirichlet Process mixture models, which make the infinite integral tractable by making assumptions which allow for using the nice analytical properties of Gaussian and Dirichlet distributions respectively.

Traditional parametric methods assume that the data is generated by simple well-known probability distributions with just a few parameters, and inference aims to determine the value of these parameters. These methods are extremely vulnerable to model misspecification. A more flexible and robust approach to parametric inference which supports a more flexible assumption on underlying distribution is to use Bayesian approximation methods such as variational inference. In variational inference, we assume  $\nu(\mathbf{x})$  to be a member of a broad family of distributions  $Q(\mathbf{c} | \mathbf{x}, \boldsymbol{\theta})$  represented by some high-dimensional parametrization-vector  $\boldsymbol{\theta}$  with a prior distribution  $p(\boldsymbol{\theta})$ , and assume that these capture most of the important variation across possible frequency distributions (Blei et al., 2016). We can for example use a neural network with weights and biases  $\boldsymbol{\theta}$  and a normalized last layer as our family of distributions  $Q(\mathbf{c} | \mathbf{x}, \boldsymbol{\theta})$ . It is then possible to incorporate the information from the training dataset  $\mathcal{D}_{\text{train}} = (\mathcal{C}_{\text{train}}, \mathcal{X}_{\text{train}})$  of size  $N_{\text{train}}$  to calculate the posterior probability

$$p(\boldsymbol{\theta} | \mathcal{D}_{\text{train}}) = \frac{p(\mathcal{C}_{\text{train}} | \mathcal{X}_{\text{train}}, \boldsymbol{\theta}) p(\boldsymbol{\theta})}{p(\mathcal{C}_{\text{train}} | \mathcal{X}_{\text{train}})} = \prod_{i=1}^{N_{\text{train}}} \frac{Q(\mathbf{c}_i | \mathbf{x}_i, \boldsymbol{\theta}) p(\boldsymbol{\theta})}{\int Q(\mathbf{c}_i | \mathbf{x}_i, \boldsymbol{\theta}) p(\boldsymbol{\theta}) d\boldsymbol{\theta}}.$$

For high dimensional  $\boldsymbol{\theta}$  or analytically intractable integrals, it is often convenient to numerically estimate the resulting integral by a crude Monte Carlo (MC) estimator with  $\{\boldsymbol{\theta}_i\}, i = 1, 2, \dots, T$ , sampled from its posterior distribution  $p(\boldsymbol{\theta} | \mathcal{D}_{\text{train}})$ , resulting in the approximation

$$\begin{aligned} P(\mathbf{c} | \mathbf{x}, \mathcal{D}_{\text{train}}) &= \int Q(\mathbf{c} | \mathbf{x}, \boldsymbol{\theta}) p(\boldsymbol{\theta} | \mathcal{D}_{\text{train}}) d\boldsymbol{\theta} = \mathbb{E}_{\boldsymbol{\theta}}[Q(\mathbf{c} | \mathbf{x}, \boldsymbol{\theta})] \\ &\approx \frac{1}{T} \sum_{t=1}^T Q(\mathbf{c} | \mathbf{x}, \boldsymbol{\theta}_t) = \bar{Q}(\mathbf{c} | \mathbf{x}, \mathcal{D}_{\text{train}}). \end{aligned} \tag{4}$$

The variance of the posterior distribution can also be approximated in a similar way:

$$\text{Var}_{\theta}[Q(\mathbf{c}|\mathbf{x}, \boldsymbol{\theta})] \approx \frac{1}{T} \sum_t^T (Q(\mathbf{c}|\mathbf{x}, \boldsymbol{\theta}_t) - Q(\mathbf{c}|\mathbf{x}, \mathcal{D}_{\text{train}}))^2 = u_Q(\mathbf{c}|\mathbf{x}, \mathcal{D}_{\text{train}})^2 \quad (5)$$

This quantity measures the spread of the estimated posterior, and it's square root,  $u_Q$ , is what we use to quantify class probability uncertainty in this study. As the inference procedure should make the posterior converge towards the LRFD, the uncertainty should in general decrease with larger datasets, and may approach zero.

### 3 Methodology

In this study, we have created synthetic data representative of a generic two dimensional binary classification problem. We have specifically focused on a task with continuous, non-Gaussian, non-periodic unbounded underlying distributions of the features with significant overlap between classes. The simplicity of the data is intentional, aiming to facilitate an in-depth examination of the algorithms rather than the data itself. Toy models are highly idealized and extremely simplified models which are a frequently used but perhaps underappreciated tool employed by natural scientists (Reutlinger et al., 2018). While toy models may not always be very useful for solving specific complex problems, they provide an excellent basis for testing basic assumptions and increase understanding. They are frequently used in statistical modeling studies but are less commonly seen in modern deep learning literature. It should be noted that the classification task is not trivial even if it is low dimensional. The class probability depends on the input features in a geometrically symmetric way, which none of the models can easily represent. The primary motivation for using toy data in this study is that by knowing the precise expression for the joint probability and the associated class probabilities as functions of the data features, we can exactly evaluate the estimates produced by the machine learning algorithms.

We investigated six different ML classification algorithms with probability and uncertainty estimates: neural network ensemble (NNE), neural network ensemble with conflictual loss (CL) (Fellaji et al., 2024), neural network using evidential deep learning (EDL) (Sensoy et al., 2018), neural network with Monte Carlo Dropout (MCD) (Gal and Ghahramani, 2016), Gaussian Process classification (GP) (Rasmussen and Williams, 2006) and a Dirichlet Process Mixture Model (DPMM) (Li et al., 2019). Four are deep learning algorithms while the other two are nonparametric Bayesian inference models. Details of the class probability and uncertainty estimation as well as extensive hyperparameter sweeps for each algorithm can be found in Appendices A and B.

#### 3.1 Research questions and evaluation metrics

Our first research question is if estimated probabilities are calibrated. This has been studied thoroughly and different metrics of calibration such as expected calibration error (Naeini et al., 2015; Guo et al., 2017; Minderer et al., 2021) have been devised. However, the majority of these studies are done on data where the LRFD is not known and must be approximated using binning schemes on finite test data. In our case, Q1 can be investigated by comparing the probability estimates for our test set (by default in-distribution data) with

the LRFD of the data. Because of the symmetries of a binary classification problem where  $P(c^1 = 1|\mathbf{x}) = 1 - P(c^2 = 1|\mathbf{x})$  we will only show the results for class 2. The differences are evaluated by plotting the estimates next to the LRFD and by calculating five summary statistics of calibration on the test set, specifically

- Z: The difference between the average estimated probability and the accuracy (Pernot, 2023);
- WD: The Wasserstein-1 distance (WD) between the estimated distribution and the LRFD (Ramdas et al., 2017);
- ECE: The expected calibration error (ECE) (Naeini et al., 2015), which is a rough approximation of the WD;
- Mean KL-div: The mean Kullback-Leibler (KL) divergence between the estimated distribution and the LRFD (Jordan et al., 1999);
- LogLoss: The cross entropy loss, which is a crude Monte Carlo approximation of the non-constant term of the KL divergence (Botev et al., 2013).

The second research question aims to answer if the uncertainties produced by the algorithms actually decrease when we increase the number of data points. In the study of Fellaji et al. (2024), where ensembles with conflictual loss are introduced, the authors call this the data-related principle of epistemic uncertainty and find NNE, MCD and EDL to not follow this principle, which is the motivation for their introduction of the CL algorithm. To evaluate if this is the case for our data, we use the average of the uncertainty estimates over the whole test set as a metric. Because of the stochastic nature of both data and training, we expect this metric to fluctuate, but it should in general go down as we add more data to the machine learning models.

The last research question is related to generalization and the ability of flexible models to make sensible predictions outside the training distribution. Ideally, we would want our uncertainty estimates to be high for data which is very different from the data previously seen by the learning algorithm (Hein et al., 2019). In our case, this means that we tested to see if probability estimates approached 0.5 and uncertainty was high in the tails of our distribution. We evaluate this by calculating the average probability estimates and uncertainty on an extrapolation test set, as well as looking at the behavior of estimates in the tails of the in-distribution test set.

## 4 Dataset and experiment

Each data point  $d$  consists of features  $\mathbf{c} \in \{[1, 0], [0, 1]\}$ , and  $\mathbf{x} = [x^1, x^2] \in \mathbf{R}^2$  with polar coordinates  $r = \sqrt{(x^1)^2 + (x^2)^2}$  and  $\phi = \arctan(x^2/x^1)$ . To facilitate visual interpretation we have chosen a distribution with radial symmetry.  $\mathbf{x}$  is distributed such that  $p(r|c^j = 1) = \Gamma(\alpha_j, \eta_j, r)$ , where  $\Gamma$  is the gamma distribution with shape parameter  $\alpha$  and scale parameter  $\eta$ . The angular density  $p(\phi|c^j = 1) = 1/2\pi$  for both classes. Two different classification datasets, dataset A and dataset B, were generated by setting the parameters of the gamma distributions to different values. For dataset A the parameter values are  $\alpha_1, \eta_1 = [2, 5]$ ,

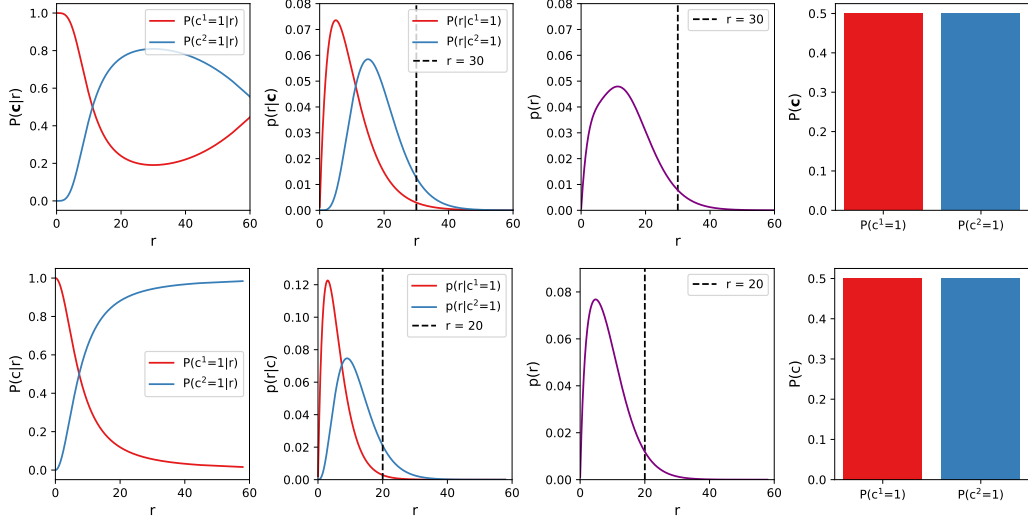


Figure 1: The conditional and marginal distributions for the two datasets. The upper row shows the distribution from which we sampled dataset A, with parameters  $\alpha_1, \theta_1 = [2, 5]$ ,  $\alpha_2, \theta_2 = [6, 3]$ . The lower row shows the distribution from which we sampled dataset B, with parameters  $\alpha_1, \theta_1 = [2, 3]$  and  $\alpha_2, \theta_2 = [4, 3]$ . The panels from left to right show the conditional distributions  $P(c|r)$ ,  $p(r|c)$ , and the marginal distributions  $p(r)$  and  $P(c)$ .

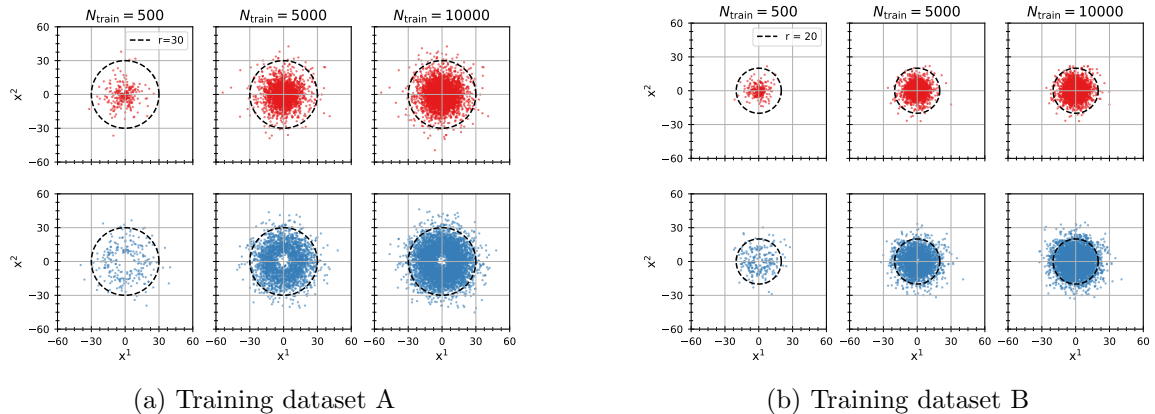


Figure 2: Subsets of the training dataset with  $N_{train} = 250, 5000$  and  $10000$  data points. The upper row shows the data points of class 1 in red and the lower row shows the data points of class 2 in blue. The left panel shows dataset A and the right panel shows dataset B.

$\alpha_2, \eta_2 = [6, 3]$  where the index indicates the class, and for dataset B the parameter values are  $\alpha_1, \eta_1 = [2, 3]$ ,  $\alpha_2, \eta_2 = [4, 3]$ . The marginal class probabilities  $P(\mathbf{c})$  are uniform for both datasets. The distributions of the data are shown in Figure 1. These specific distributions were chosen because of the different behavior for  $P(\mathbf{c}|r)$  in the beginning of the tails, around  $r = 30$ . Train, validation and test sets with 10000, 5000, and 10000 samples, respectively, were generated. To check estimated probabilities and uncertainties for OOD test points, a grid in polar coordinates was created by letting  $\phi_i \in \{0, \frac{2}{5}\pi, \frac{4}{5}\pi, \frac{6}{5}\pi, \frac{8}{5}\pi\}$  and  $r_i$  be 26 equally-spaced values in log-space between 700 and 1000 for each polar angle, resulting in 130 data points.

Each model was trained on the same subsets of increasing amounts of training data with  $N_{\text{train}} = 250, 500, 1000, 2000, 3000, 5000$  and 10000. Figure 2 shows the training data for 250, 1000 and 10000 training points. As the gradient descent optimization algorithm is sensitive to initialization values of its parameters and the order in which training data is seen, 20 separate training runs were performed for each NN algorithm and the one with the lowest cross entropy loss on the validation set was kept. The trained models were then used to estimate the class probability and uncertainty on the test set and the extrapolation grid. Details on training and implementation can be found in Appendix A.

## 5 Results

In this section we present the results of the experiment and how they relate to each research question.

### 5.1 Calibration results

First we attempt to answer Q1 by evaluating if the estimated probabilities fluctuate around the LRFD and approach it as we increase the amount of training data. Figure 3 and Figure 4 shows the estimated probabilities  $\bar{Q}(c^2 = 1|\mathbf{x})$  and uncertainties  $u_Q(c^2 = 1|\mathbf{x})$  as a function of polar coordinate radius  $r = |\mathbf{x}|$  with error bars indicating the entire spread of estimates over polar angle  $\phi$ , calculated on the test set of each of the six algorithms from training on 500 and 5000 training data points from dataset A and B respectively. The figures show that probability estimates are well calibrated for all algorithms from around  $0 \leq |\mathbf{x}| \leq 30$  for dataset A and  $0 \leq |\mathbf{x}| \leq 20$  for dataset B. As we add more training data, the estimates concentrate around the LRFD and the error bars shrink. From around  $|\mathbf{x}| \geq 30$  and  $|\mathbf{x}| \geq 20$  for dataset A and B respectively, some of the estimates do not fluctuate around the LRFD and are no longer calibrated, which becomes more apparent as we move further away from the bulk of the training data. The behavior in the tails is further covered in the results of Q3.

Figure 5 shows the five different calibration-related summary statistics as well as the global accuracy calculated on the test set as a function of increasing number of training data points. The plots show that all models converge towards the LRFD as the data size increases, but the metrics are quite noisy and do not always give the same relative ranking to each model. The neural networks are trained specifically to minimize the cross entropy loss and a decrease in this metric does not always correspond to a decrease in for example estimated calibration error or even KL divergence. For dataset A, the GP model scores are better relative to many of the other models, as the LRFD of that dataset aligns better with

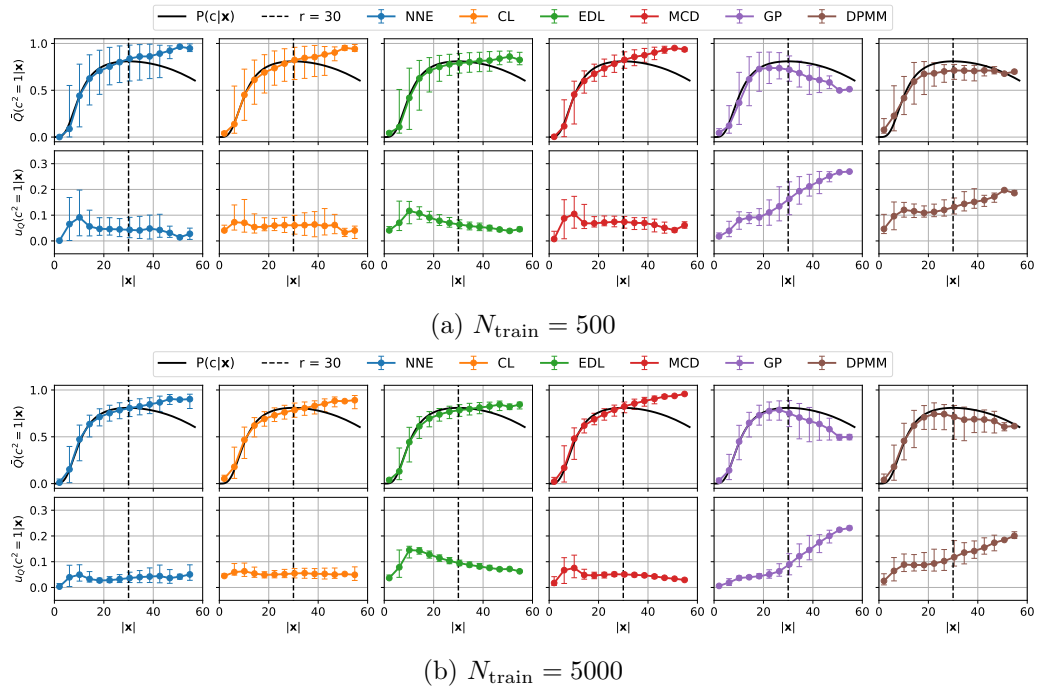


Figure 3: Estimated probabilities (top row) and uncertainties (bottom row) for class 2 for the different algorithms for dataset A as a function of radius  $|x|$ . The error bars indicate the entire spread of the data over polar angle  $\phi$ . The long-run frequency distribution (solid black line) is plotted for reference.

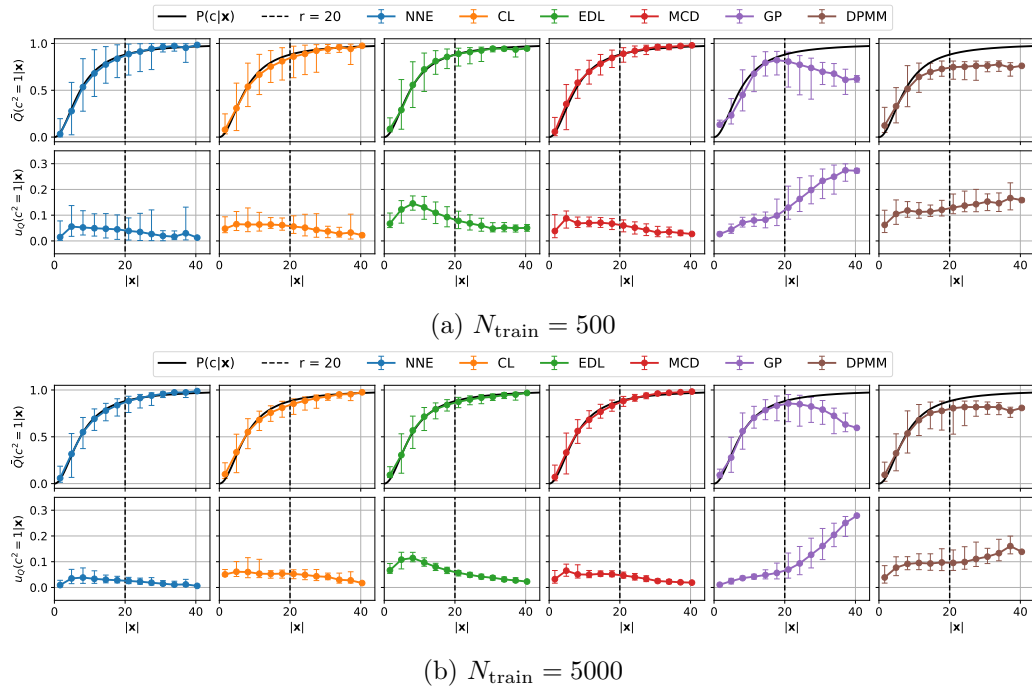


Figure 4: Estimated probabilities (top row) and uncertainties (bottom row) for class 2 for the different algorithms for dataset B as a function of radius  $|x|$ . The error bars indicate the entire spread of the data over polar angle  $\phi$ . The long-run frequency distribution (solid black line) is plotted for reference.

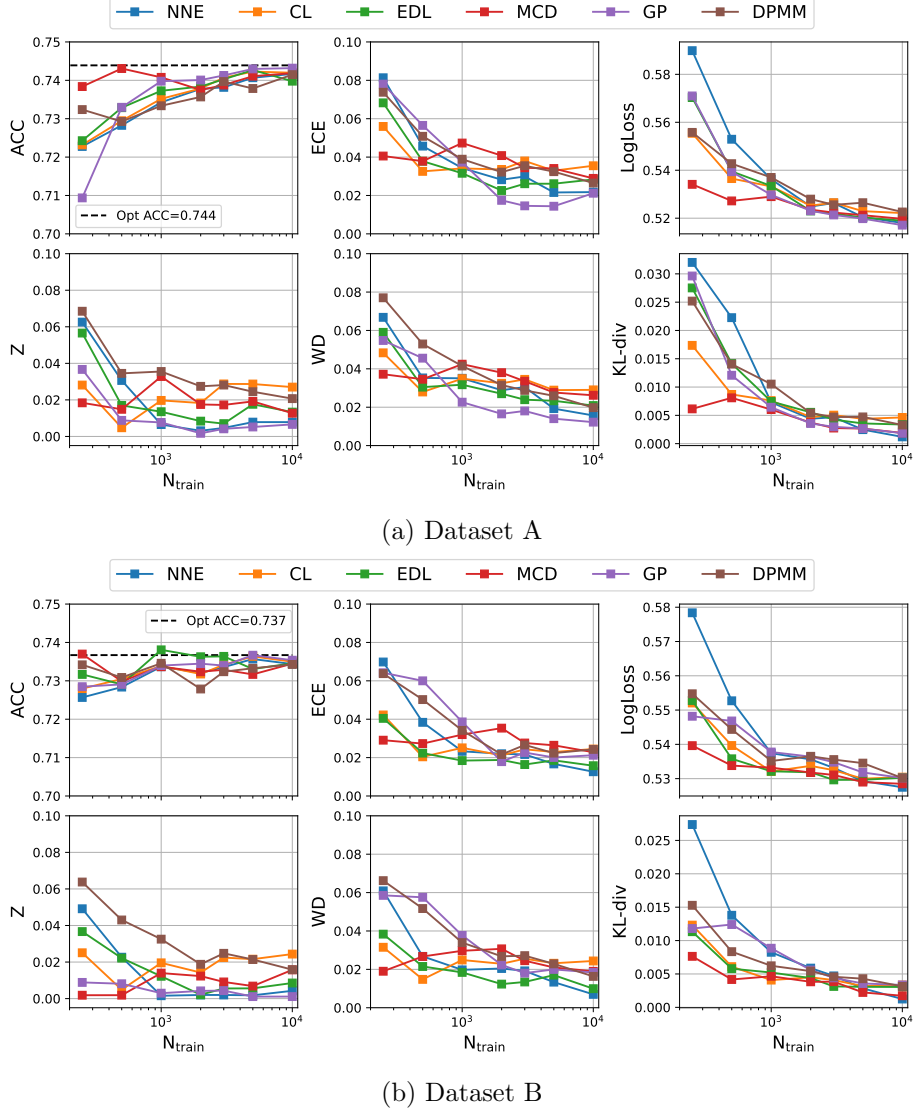


Figure 5: Calibration metrics of the test set as a function of number of training data points  $N_{\text{train}}$ . The six subplots show the scores of the different models: neural network ensemble (NNE, blue line), neural network ensemble with conflictual loss (CL, orange line), neural network using evidential deep learning (EDL, green line), neural network with Monte Carlo Dropout (MCD, red line), Gaussian Process classification (GP, purple line) and a Dirichlet Process Mixture Model (DPMM, brown line). The metrics calculated are the accuracy (ACC), estimated calibration error (ECE), cross entropy loss (LogLoss), model calibration error (Z), Wasserstein-1 distance (WD) and Kullback-Leibler divergence (KL-div). The dashed black line in the top left plot indicates the optimal accuracy of the test set.

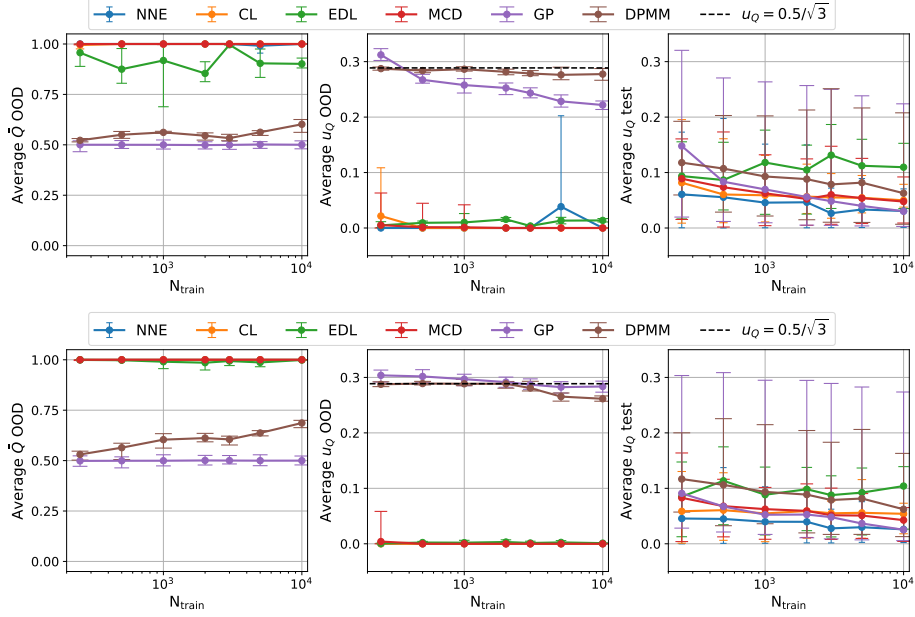


Figure 6: Top: Average estimated out-of-distribution probabilities (left), out-of-distribution uncertainty (middle) and test set uncertainty (right) as a function of  $N_{\text{train}}$  for dataset A (top row) and B (bottom row). The error bars indicate the entire spread of the data over polar angle  $\phi$ . The colors are similar to Figure 5. The dashed black line in the middle plot indicates the standard deviation of the posterior of a Bernoulli distribution with one data point of class 2 with prior Beta(1, 1).

the prior (bias) of the GP. For dataset B the opposite is true. These plots also illustrate that estimated calibration error and cross entropy loss, which are evaluated using only the labels of the test set and not the LRFD can be fairly good estimates of the usually intractable Wasserstein-1 distance and mean KL-divergence metrics (if the test set is large enough).

## 5.2 Data-size dependency for uncertainty results

Next we investigate Q2 by checking if the uncertainties for both in-distribution and OOD data goes down as we increase the training data size. Figure 6 shows the average estimated probabilities and uncertainties for the OOD test points with  $700 < |\mathbf{x}| < 1000$  as well as average uncertainties for the in-distribution test set as a function of increasing number of training data points. For the OOD test points, all algorithms except for GP and DPMM produce approximately constant uncertainties. The standard deviation of the posterior of a Bernoulli distribution with one data point of class 2 with prior Beta(1, 1), as described by Equation 3 is also plotted for comparison. GP uncertainties decrease, which is due to the calculated approximate optimal value for the output variance of the Radial Basis Kernel decreasing with increasing nr of data points (see Appendix A). The DPMM uncertainties may decrease due to numerical errors because of increasingly small probability density estimates in the tail, as expanded on in the next results section. For all algorithms except EDL, the uncertainties on the test set tend to go down as we increase the size of the

training set. For EDL however, the uncertainties increase and for dataset B, CL average uncertainties stay almost constant as we increase the data size.

### 5.3 Tail estimates and out-of-distribution probability and uncertainty results

Finally we answer Q3 by checking if uncertainty estimates increase as we move away from the bulk of the training data. We go back to examining Figure 3 and Figure 4, with a focus on the tails, defined loosely to be  $|\mathbf{x}| \geq 30$  and  $|\mathbf{x}| \geq 20$  for dataset A and B respectively. For dataset A, the neural network-based algorithms tend to first underestimate the class 2 probabilities, then overestimate them. For dataset B, they almost perfectly align with the LRFD. The nonparametric Bayesian inference algorithms on the other hand underestimate the probabilities in the tails relative to the LRFD for both datasets, giving estimates closer to the noninformative prior probability estimate of 0.5. The spread over polar angles of the estimates (the height of the error bars in the plot) as a function of increasing amounts of data in this data range also differ between the neural network and the nonparametric Bayesian models. The neural network models have error bars that shrink with increasing amounts of data regardless of whether the estimates are close or not to the LRFD, while the nonparametric Bayesian models have error bars that do not shrink (the DPMM error bars even grow) for test points in the tails. The uncertainty estimates of all algorithms approximately follow the estimated probabilities in the calibrated areas as the standard deviation of the estimated frequency of a Bernoulli distribution is proportional to  $\sqrt{\nu(1 - \nu)}$ , which results in a local maxima around  $\nu = 0.5$ . The height of this maxima is different for all the models, indicating that the uncertainty values are highly model dependent. In the tails of the test set distribution, uncertainties increase for the nonparametric Bayesian models. The neural network models have flat or decreasing uncertainties in the tail.

The first two panels of Figure 6 show the average estimated probabilities and uncertainties on the OOD datasets. For most deep learning models, the probability estimates are approximately 1. The only exception is EDL which for dataset A has very noisy estimates centered around 0.9. The NN-algorithms all also have estimated uncertainties of approximately 0. This is the correct value for a variance proportional to  $\sqrt{\nu(1 - \nu)}$  when  $\nu$  is 0 or 1, and so does not indicate that there is some fundamental error in the approximation of the variance of the distribution. The exception is the NNE uncertainty estimates for dataset A  $N_{\text{train}} = 5000$  which are non zero and extremely noisy. This anomaly corresponds to diverging estimates in the ensemble, which seems to be a rather unusual result when the ensemble is trained well. The NN models therefore do not show a strong, consistent increase in uncertainty with decreasing density  $p(\mathbf{x})$ . The GP algorithm produces probability estimates of approximately 0.5 and high uncertainty for OOD data points for both datasets independent of data size. The DPMM algorithm also produces high uncertainty for OOD data and OOD probability estimates close to 0.5 for the smallest amount of training data, but the probability estimates diverge from 0.5 as we increase the number of data points, pushing the estimated distribution towards 1. This is unexpected as the expected out-of-distribution frequency of a Bernoulli distribution using the Bayes-Laplace (uniform) prior as our DPMM algorithm does, should give an estimate of 0.5. To calculate the conditional distribution however, the algorithm actually approximates the joint distribution, which gives very small probabilities for the data in low density areas. The results may therefore be influenced by

biased numerical errors or possibly pathologies of the underlying mathematical framework (Dunson and Bhattacharya, 2011).

To study the effect of hyperparameter choice on our deep learning results we have performed a grid search over relevant hyperparameters such as the size of the neural networks, the learning rate, the weight decay and some algorithm specific hyperparameters. Detailed results are presented in Appendix B. We find that some settings of hyperparameters give rise to non-extreme OOD probability estimates, but these correspond to networks that have not learned well and perform badly on the in-distribution test set. The majority of the trained networks result in extreme probability estimates similar to the ones presented in the main part of the study. Some of the hyperparameter choices also give rise to higher OOD uncertainty than in the main findings. These are also connected to networks that perform worse and often significantly so. All in all, our grid search corroborates our main findings and provide some interesting additional information on the behavior of the algorithms.

As an additional test we performed the same experiments with a dataset with two identically distributed classes. Predictions on OOD data from NNE, CL and MCD varied greatly for different polar angles. For small learning rates, EDL estimated probabilities close to 0.5 and uncertainty close to 0. GPs also estimated probabilities close to 0.5 and uncertainty close to 0, while DPMMs estimated probabilities close to 0.5 and uncertainties close to 0.3. For more information see Appendix C.

## 6 Discussion and conclusion

To sum up, in the case of our data

- the algorithms studied are all fairly well calibrated for in-distribution data where comparisons with the long-run frequency distribution make sense;
- the average uncertainty on the test set go down as we increase the number of training data points for all algorithms except evidential deep learning which go up, indicating that something might be wrong in assumptions or implementation;
- the out-of-distribution average uncertainty as a function of number of training data points is high and goes down for the Gaussian process classifier and Dirichlet process mixture model, and is low or zero and constant for the deep learning models;
- for out-of-distribution data all deep learning algorithms estimated extreme probabilities, while the nonparametric Bayesian models estimate probabilities around 0.5, with the Dirichlet process mixture model estimating slightly higher probabilities as the number of training data points increase, indicating some numerical instability or other error in implementation.

The DPMM is explicitly defined as having a  $\text{Beta}(1, 1)$  prior for class probability, and results support the qualitative correctness of the approximate posterior. For the neural networks and GP, the prior is implicitly defined, and so it is harder to evaluate the cohesiveness of the results. It is possible to interpret the deep learning results as representative of approximate posterior distributions with  $\text{Beta}(0, 0)$  priors for class probability. This suggests that changing the implicit prior for the deep learning models through modifying the loss function could change the observed behavior. However, it might not be a good idea to assign

those kind of interpretations post-hoc, as we might put too much trust in a method without a principled theoretical foundation. Instead, we might consider if the approximations introduced by variational inference are the cause of the deviation from desired results.

Although neural networks with rectified linear (ReLU) activation functions can in theory approximate any nonlinear function of the data locally, they eventually become simple linear functions of the input features if one moves in any direction far enough (Hein et al., 2019). This property of piecewise linear neural networks, combined with using the softmax function for normalization of the last layer of the network, gives rise to class probabilities that asymptotically approach extreme values of zero or one. Therefore the estimated extreme probabilities for out-of-distribution data may simply be a feature of using ReLU neural networks as the family of parameterized test distributions in variational inference. Similar to more well known parametric methods such as linear regression we should not expect our model to be informative or correct if we extrapolate too far. Changing the architecture and activation functions to better reflect the kind of statistical model we seek is an obvious step to mitigate the problem of model misspecification.

It might also be the case that taking the shortcut of directly calculating the conditional class probabilities through supervised learning methods will never give us uncertainties that are dependent on the joint probability density. In that case, anomaly detection or other density estimation methods (such as the DPMM in this study) are obvious choices for estimates which warn about out-of-distribution data. Further studies, both empirical and theoretical, are needed to investigate these pathologies of neural networks and the effect of changing important elements like the activation function. There also exists many more algorithms for class probability estimation with uncertainties, such as different approximations of Bayesian neural networks, and looking into these is a topic for future research.

This study only investigates data which is sampled from a relatively simple two dimensional distribution and therefore does not represent the complexities present in real-world data. It is noteworthy that even for this relatively simple problem, many of the learning algorithms do not produce uncertainties which can be used by scientists to decide if they should trust the estimates. Although the uncertainty estimates produced by the deep learning algorithms presented in this study were not especially useful for this type of data, they might work better for data with for example discrete or bounded distributions, or for data with statistically independent input features. We strongly recommended that scientists create their own toy data that more closely matches the mathematical properties of their own data of interest to see how the different machine learning algorithms can be expected to behave in their case.

Regardless of the mathematical reason for the observed behavior and the inherent limitation of empirical studies, we can take away some key lessons from the experiment. Deep learning-based class probability estimates and uncertainties do not necessarily exhibit the behavior we expect or desire for out-of-distribution data. This may be partly due to a lack of understanding of what can reasonably be expected from a statistical method, like the fact that it is not possible to have unbiased frequency estimates which also extrapolate to a specific value in the  $N \rightarrow 0$  limit. It can also be because we do not yet have a clear understanding of the implicit statistical models we create or the inherent limitations of the approximations we make in our inference algorithms to facilitate faster learning and compute intractable integrals. In any case, this study should serve as a reminder that purely

data-driven complex statistical models and learning algorithms should not be trusted out of the box. Sanity checks with intuitive toy-problems such as this one are a useful tool to explore the way these algorithms behave, and we hope this study can serve as an inspiration and a guide for future machine learning development work in the natural sciences.

### **Acknowledgments and Disclosure of Funding**

We acknowledge support from the Research Council of Norway, grant no 314472, which is supporting the research of A.G.

## Appendix A. Algorithms

In this section we describe the theoretical interpretation as well as any assumptions and computational details of the six algorithms used in the study.

### A.1 Neural networks with stochastic gradient descent

A simple approximation of the posterior distribution of variational inference may be obtained by assuming that only the value  $\boldsymbol{\theta} = \boldsymbol{\theta}_{\max}$  which maximizes the posterior  $p(\boldsymbol{\theta}|\mathcal{D}_{\text{train}})$  contributes significantly to the integral in Equation 4. This assumption holds if there is just one mode, which is close to the mean and most of the probability mass is centered around it. This is the case if we assume the posterior to be approximately Gaussian. The maximum a posteriori estimate may be found by any optimization method which can maximize the posterior with respect to  $\boldsymbol{\theta}$ . In the case of deep learning we use stochastic gradient descent derived optimization techniques for expectation maximization with regularization, which may be interpreted in a Bayesian way as sampling from this assumed Gaussian-like posterior distribution as defined by the NN architecture and the stochastic gradient descent algorithm and hyperparameters (Duvenaud et al., 2016).

All deep learning algorithms were implemented in `pytorch`.

### A.2 Neural Network ensembles

In neural network ensemble models we independently train  $N_E$  number of ensembles to get a set of samples  $\hat{\boldsymbol{\theta}}_{\max,i}$  from the posterior distribution and use these to compute the estimated probability and uncertainty using Equations 4 and 5 as

$$\bar{Q}_{\text{NNE}}(\mathbf{c}|\mathbf{x}, \mathcal{D}_{\text{train}}) = \frac{1}{N_E} \sum_{i=1}^{N_E} Q(\mathbf{c}|\hat{\boldsymbol{\theta}}_{\max,i}, \mathbf{x}),$$

and

$$u_{\text{NNE}}^2(\mathbf{c}|\mathbf{x}, \mathcal{D}_{\text{train}}) = \frac{1}{N_E} \sum_{i=1}^{N_E} (Q(\mathbf{c}|\hat{\boldsymbol{\theta}}_{\max,i}, \mathbf{x}) - \bar{Q}_{\text{NNE}}(\mathbf{c}|\mathbf{x}, \mathcal{D}_{\text{train}}))^2.$$

### A.3 Conflictual loss

Conflictual loss (CL) is an algorithm proposed by Fellaji et al. (2024) which aims to give the ensemble uncertainties the property of being higher where there is little data and lower for network ensembles with fewer parameters. This is done by biasing an equal number of networks in the ensemble towards each class by adding a “fake data”-term to the loss function

$$L_{\text{CL},i}(\mathcal{D}_N, \boldsymbol{\theta}) = \text{CE}(\mathcal{D}_N, \boldsymbol{\theta}) - \sum_{i=1}^N \sum_{j=1}^k \beta \log Q(c^b = 1|\boldsymbol{\theta}, \mathbf{x}_i)). \quad (6)$$

Here  $i$  is the index of the network in the ensemble,  $b$  is the index of the class that network is biased towards and  $\beta$ , the bias weight, is a hyperparameter which governs the strength of the bias.

The cross entropy loss of  $N$  data points is given by

$$\text{CE}(\mathcal{D}_N, \boldsymbol{\theta}) = - \sum_{i=1}^N \sum_{j=1}^k c_i^j (\log Q(c^j = 1 | \boldsymbol{\theta}, \mathbf{x}_i)).$$

The estimated probability and uncertainty is calculated as in NNE. This method can be seen as an attempt at indirectly changing the strength of the bias in Equation 2.

#### A.4 Monte Carlo Dropout

In deep learning using Monte Carlo Dropout (MCD) for uncertainty estimation (Gal and Ghahramani, 2016), the “dropping out” of weights commonly used during training to prevent overfitting, is applied at both training and inference phases. Specifically, during each forward pass through the network, random weights are set to zero according to a specified hyperparameter referred to as the dropout rate. MCD is related to ensemble learning. By performing multiple forward passes with different dropout masks, we generate a distribution of networks with associated predictions for a given input. Using a neural network with one infinitely wide hidden layer and MCD can theoretically be shown to be equivalent to a Gaussian Process, and therefore MCD is frequently referred to as approximate Bayesian inference. The estimated MCD probabilities and uncertainties presented in this study are the sample mean and standard deviations of 500 forward passes through the network.

#### A.5 Evidential deep learning

Evidential deep learning (EDL), as presented by (Sensoy et al., 2018) which is based on the mathematical framework of subjective logic, replace the class probability point estimates of a neural network classifier trained on  $k$  classes with a Dirichlet density distribution

$$D(\boldsymbol{\nu} | \boldsymbol{\alpha}) = \frac{1}{B(\boldsymbol{\alpha})} \prod_{i=1}^k (\nu^i)^{\alpha^i - 1},$$

where the components of  $\nu$  belong to the standard  $k-1$  simplex and  $B(\boldsymbol{\alpha})$  is the multivariate beta function.  $\alpha^j = e^j + 1$  where  $e^j$  is the “evidence”, in this case  $e = \text{softplus}(x) = \log(1 + \exp(x))$  of the logit outputs  $\mathbf{f}(\mathbf{x}, \boldsymbol{\theta}) \in \mathbf{R}^k$  of the last non-softmax layer of the deep neural network.

The network is trained using the loss function

$$\begin{aligned} L_{\text{EDL}}(\mathcal{D}_N, \boldsymbol{\theta}) = & \sum_{i=1}^N \sum_{j=1}^k c_i^k (\psi(S(\mathbf{x}_i)) - \psi(\alpha(\mathbf{x}_i)_i^j)) + \\ & \lambda(t) \sum_{i=1}^N \text{KL}[D(\boldsymbol{\nu}_i | \boldsymbol{\alpha}(\tilde{\mathbf{x}}_i)_i || D(\boldsymbol{\nu}_i | \langle 1, \dots, 1 \rangle)], \end{aligned}$$

where  $S_i = \sum_{k=1}^k \alpha_i^k$  and  $\tilde{\boldsymbol{\alpha}} = \mathbf{c}_i + (1 - \mathbf{c}_i) \cdot \boldsymbol{\alpha}(\mathbf{x}_i)$ . This is the sum of the Bayes risk and the weighted KL-divergence between the estimated distribution and the uniform

Dirichlet distribution. The weight  $\lambda(t)$  determines the strength of the second term, and is usually implemented as a linear function of the current epoch during training. In our case  $\lambda(t) = \lambda_0 t / 200$  and  $\lambda_0$  is a hyperparameter. The training algorithm aims to ensure that data points with no evidence are assigned a low belief mass, resulting in high uncertainty.

The estimated probabilities and uncertainties used in the study are the mean and standard deviation of the resulting distribution:

$$\bar{Q}_{EDL}(\mathbf{c}|\mathbf{x}, \mathcal{D}_{\text{train}}) = \mathbb{E}_D[\nu(\mathbf{c}|\mathbf{x})] = \frac{\alpha}{\sum_{i=1}^K \alpha^i}$$

$$u_{EDL}^2(\mathbf{c}|\mathbf{x}, \mathcal{D}_{\text{train}}) = \text{Var}[\nu(\mathbf{c}|\mathbf{x})] = \frac{\mathbb{E}[\nu(\mathbf{c}|\mathbf{x})](1 - \mathbb{E}[\nu(\mathbf{c}|\mathbf{x})])}{\sum_{i=1}^K \alpha^i + 1}.$$

Our implementation of EDL is taken from the original paper’s GitHub repository<sup>2</sup>.

## A.6 Nonparametric Bayesian Machine Learning

Nonparametric Bayesian inference algorithms provide principled methods of predictive inference for complex data. The connection between nonparametric Bayesian statistics and deep learning provides a bridge between the disciplines of statistics and machine learning and allows us to approach the latter with a well developed theoretical framework. We have included two Bayesian nonparametric inference algorithm in this study to show the similarities and differences to the approximate deep learning algorithms.

## A.7 Gaussian Process

A Gaussian Process (GP) is a Bayesian nonparametric approach to machine learning and closely related to deep learning (Rasmussen and Williams, 2006). In a GP model, we assume the relation  $y = f(x) + \epsilon_y$  where  $y$  is the variate we want to predict,  $x$  are the rest of the variates,  $f(x)$  is some function and  $\epsilon_y$  is normally distributed noise. This makes  $f(x) = y - \epsilon_y$  also normally distributed as  $\mathcal{N}(\mu_f, \sigma_f)$ , with  $\mu_f$  and  $\sigma_f$  given by the kernel function  $\kappa(x, x_*)$  whose value is dependent on the relation between the training data points  $x$  and the test point(s)  $x_*$ . In a binary classification task, the GP outputs the mean and variance of the logits  $f_* = f(\mathbf{x}_*)$  for each test point  $x_*$  which we may transform to have the properties of a binomial probability distribution through the `sigmoid` function to perform logistic regression. If we use a kernel function which diverges for  $x$  far from  $\mu_x$ , such as the radial basis function kernel, the estimated class probabilities converge towards 1/2 far from the data and the estimated uncertainties also converge towards some value decided by the implicit prior given by the chosen kernel and hyperparameters. To keep the mathematical framework consistent with the rest of the analysis and bypass the difficulty of evaluating the intractable integral caused by the sigmoid function, probabilities and standard uncertainties are approximated using  $T = 1000$  Monte Carlo samples generated from  $\mathcal{N}(\mu_{f*}, \sigma_{f*})$ <sup>3</sup>:

2. <https://github.com/clabrugere/evidential-deeplearning/tree/main>

3. The difference between these probability estimates for our test set and other approximations of the class probabilities such as the approximation by David J.C. MacKay (MacKay, 1992) or the implementation used in Scikit taken from (Williams and Barber, 1998) is less than 0.01.

Table 1: Optimal hyperparameters for the Radial Basis Function kernel of the Gaussian Process for increasing number of training data points.

(a) Dataset A			(b) Dataset B		
$N_{\text{train}}$	$l$	$\sigma_o$	$N_{\text{train}}$	$l$	$\sigma_o$
250	5.45	1.97	250	8.65	1.87
500	8.97	1.47	500	9.43	1.84
1000	8.15	1.38	1000	9.09	1.79
2000	7.58	1.34	2000	5.94	1.71
3000	7.4	1.26	3000	5.43	1.67
5000	7.24	1.14	5000	5.85	1.62
10000	7.21	1.09	10000	6.57	1.63

$$\begin{aligned}
 \mathbb{E}_{f_*}[\text{sigmoid}(f_*)] &= \int \text{sigmoid}(f_*) p(f_* | \mathcal{D}_{\text{train}}) df_* \\
 &\approx \frac{1}{T} \sum_{t=1}^T \text{sigmoid}(f_{*,t}) = \bar{Q}_{\text{GP}}(\mathbf{c} | \mathbf{x}, \mathcal{D}_{\text{train}}) \\
 u_{\text{GP}}(\mathbf{c} | \mathbf{x}, \mathcal{D}_{\text{train}})^2 &= \frac{1}{T} \sum_{t=1}^T (\text{sigmoid}(f_{*,t}) - \bar{Q}_{\text{GP}}(\mathbf{c} | \mathbf{x}, \mathcal{D}_{\text{train}}))^2
 \end{aligned}$$

with  $p(f_* | \mathcal{D}) = \mathcal{N}(\mu_{f_*}, \sigma_{f_*})$ .

We used a modified version of the `GaussianProcessClassifier` class in `scikit learn` (Pedregosa et al., 2011) to extract the mean and standard deviation of the latent function posterior distribution. A radial basis function kernel with initial output variance 2 and length scale 8 was used. These parameters are automatically optimized and are given in Table 1.

### A.8 Dirichlet Process Mixture Model

The last model in the study is a Dirichlet process mixture model (DPMM) of product kernels. The Dirichlet Process is a stochastic process which generalizes the Dirichlet distribution, the conjugate prior for a discrete nominal variate with a fixed number of categories, into the prior for infinitely many categories, making the mixture model nonparametric (Li et al., 2019). Unlike the GP, this framework makes no simplifying Gaussian assumptions, and should be able to model more complex distributions. The algorithm is also the only one in the study that approximates the full joint distribution  $p(\mathbf{c}, \mathbf{x} | \mathcal{D})$ . This makes the data model powerful but the calculations become more difficult and require extensive resource demanding Markov-Chain Monte Carlo simulations. The predictive posterior probability for a new data point is given by

$$p(\mathbf{d} | \mathcal{D}_{\text{train}}) = \int Q(\mathbf{d} | \mathbf{w}, \boldsymbol{\alpha}) dp(\mathbf{w}, \boldsymbol{\alpha} | \mathcal{D}_{\text{train}}) = \int \sum_{i=1}^M w_i \prod_{j=1}^{n+1} A_j(\mathbf{d}_j, \boldsymbol{\alpha}_{i,j}) dp(\mathbf{w}, \boldsymbol{\alpha} | \mathcal{D}_{\text{train}}),$$

where  $\mathbf{w}$  are the mixture weights,  $A_j$  are feature specific parametric distributions with mixture-dependent parameters  $\boldsymbol{\alpha}_{i,j}$ ,  $n$  is the dimensions of  $\mathbf{x}$  and  $M$  are the number of non-zero mixture components. Knowing the joint distribution lets us calculate any quantity of interest such as conditional or marginal distributions using the normal rules of probability calculus. The specific parametric family of distributions,  $A_j$ , that are attributed to each variate and their associated prior distributions influence the modeling and computational performance and should be chosen carefully, although the available choices are limited by computational and numerical restraints (Görür and Rasmussen, 2010).

For our study we used the implementation in v0.2.1 of the R-package `inferno` (Porta-Mana et al., 2024)<sup>4</sup> based on the mathematical framework of (Dunson and Bhattacharya, 2011; Ishwaran and Zarepour, 2002), which is a flexible framework for regression and classification on manifolds. The prior distribution and hyperparameter choices are kept default as described in the accompanying documentation (Porta-Mana, 2025). The most relevant hyperparameter choice is the use of a Bernoulli distribution with a Beta(1, 1) prior for the class variate. Changing the value of the Beta hyperparameters corresponds to changing the strength of our “noninformative” belief of equal probability in each class. 1200 samples of  $\mathbf{w}, \boldsymbol{\alpha}$  for the approximation of the joint posterior distribution were collected using Gibbs sampling and 10 Markov-Chain Monte Carlo chains with a burn-in of 3600 samples and early stopping (Gong and Flegal, 2016). We approximate the expected value and standard uncertainty of the conditional class probability by the sample mean and standard deviation of the conditional class probabilities calculated from the Monte Carlo samples.

$$\bar{Q}_{\text{DPMM}}(\mathbf{c}|\mathbf{x}, \mathcal{D}_{\text{train}}) = \frac{1}{T} \sum_{t=1}^T Q(\mathbf{c}|\mathbf{x}, \mathbf{w}_t, \boldsymbol{\alpha}_t)$$

$$u_{\text{DPMM}}^2(\mathbf{c}|\mathbf{x}, \mathcal{D}_{\text{train}}) = \frac{1}{T} \sum_{t=1}^T (Q(\mathbf{c}|\mathbf{x}, \mathbf{w}_t, \boldsymbol{\alpha}_t) - \bar{Q}_{\text{DPMM}}(\mathbf{c}|\mathbf{x}, \mathcal{D}_{\text{train}}))^2$$

## Appendix B. Neural network hyperparameters

The neural networks we have used in the study are all fully connected neural networks with ReLU activation functions. Changing the activation function does seem to change the extrapolation values of the estimated probabilities and uncertainties, but we choose to focus on the ReLU activation function as it is the most widely used in deep learning. They are trained using stochastic gradient descent with the AdamW modification of the Adam optimizer(Kingma and Ba, 2015) so we could control the weight decay. The models are trained on batches of [128, 128, 256, 256, 1024, 1024, 2048] samples for  $N_{\text{train}} = [250, 500, 1000, 2000, 3000, 5000, 10000]$ . The models were each trained for a maximum of 200 epochs (substantially more than needed) with early stopping if the loss did not decrease within 20 epochs.

A grid search was run over hyperparameter settings where we investigated the influence of changing learning rate (0.01, 0.001 and 0.0001), weight decay (0.1, 0.01 and 0.001) and network size (1, 3, 8 hidden layer(s) with 20, 200, 2000 nodes respectively) as well as the

---

4. <https://github.com/pglpm/inferno/>

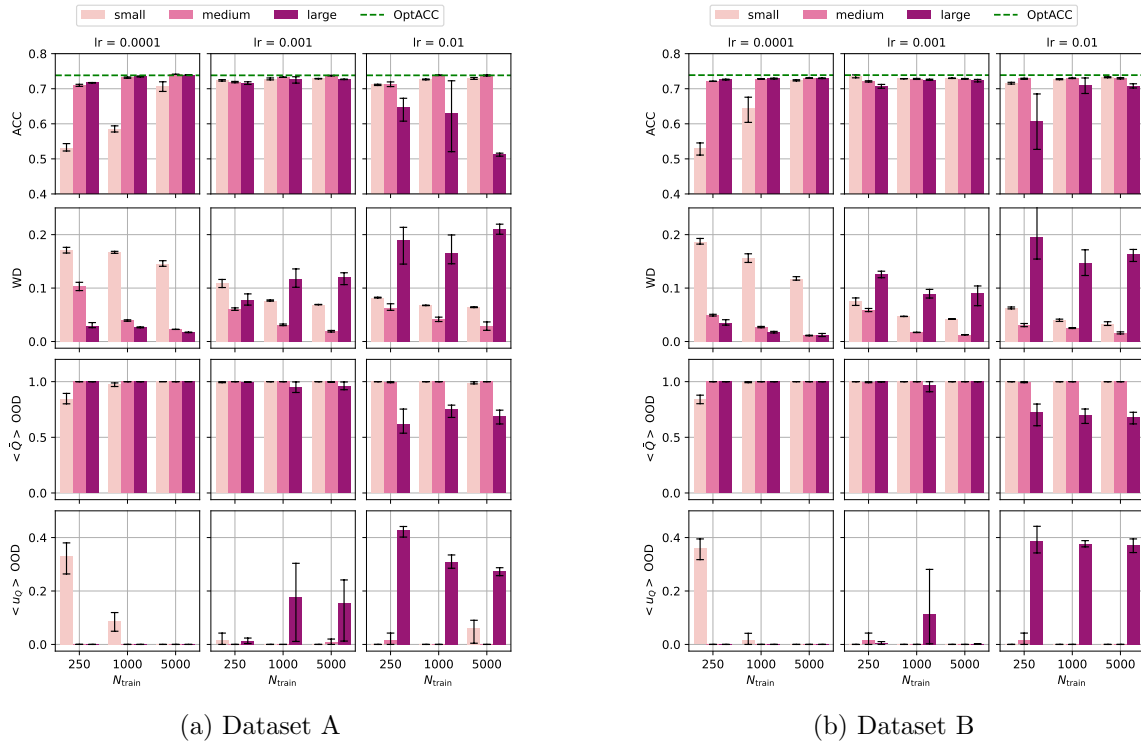


Figure 7: Results for different hyperparameter settings for neural network ensemble (NNE). The columns contain the results for learning rates 0.0001, 0.001 and 0.01. The color of the bars indicates the depth and width of the hidden layers of the network. Small, medium and large has 1, 3, and 8 hidden layers with 20, 200 and 2000 nodes respectively. The top row plots shows the accuracy on the validation set, with the green dashed line indicates the optimal accuracy for that validation set. The second row plots shows the Wasserstein distance (WD) of the validation set. The two last rows of plots show the average estimated class probability and uncertainty for out-of-distribution test points. The error bars indicate the 2.5-97.5 percentiles.

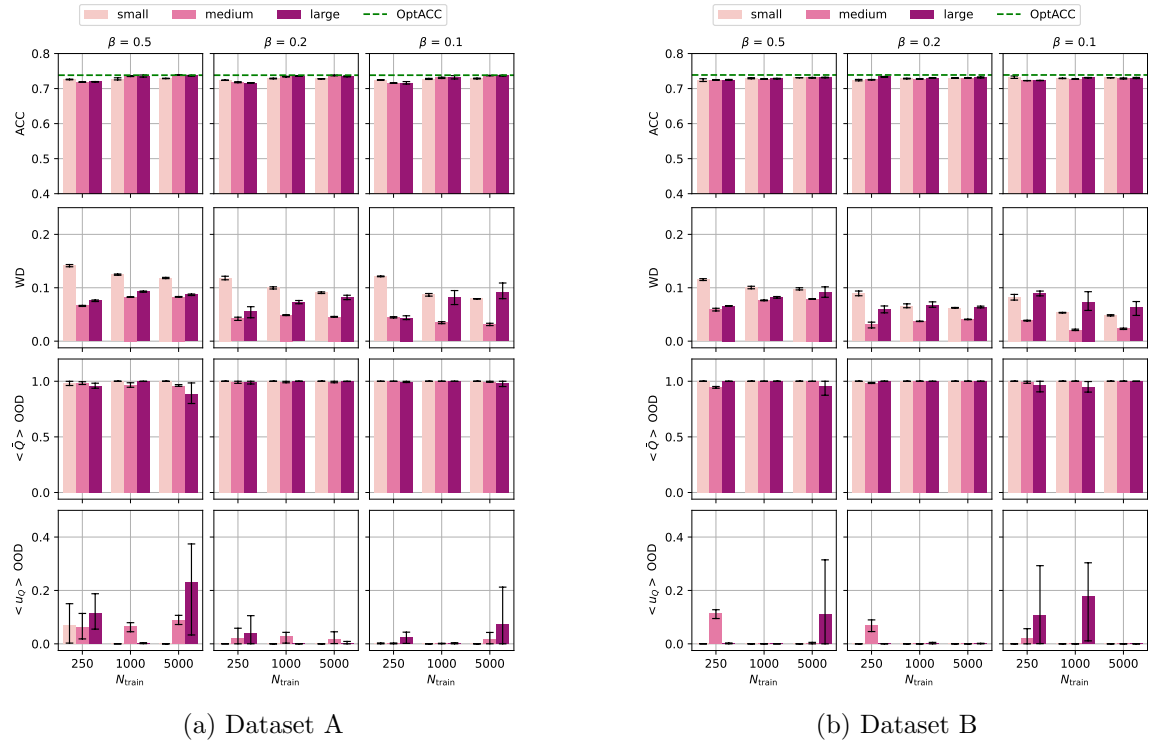


Figure 8: Results for different hyperparameter settings for neural network ensemble with conflictual loss (CL). Same as for Figure 7 except all the models are trained with learning rate 0.001 and the columns show results for different values of the bias weight  $\beta$ .

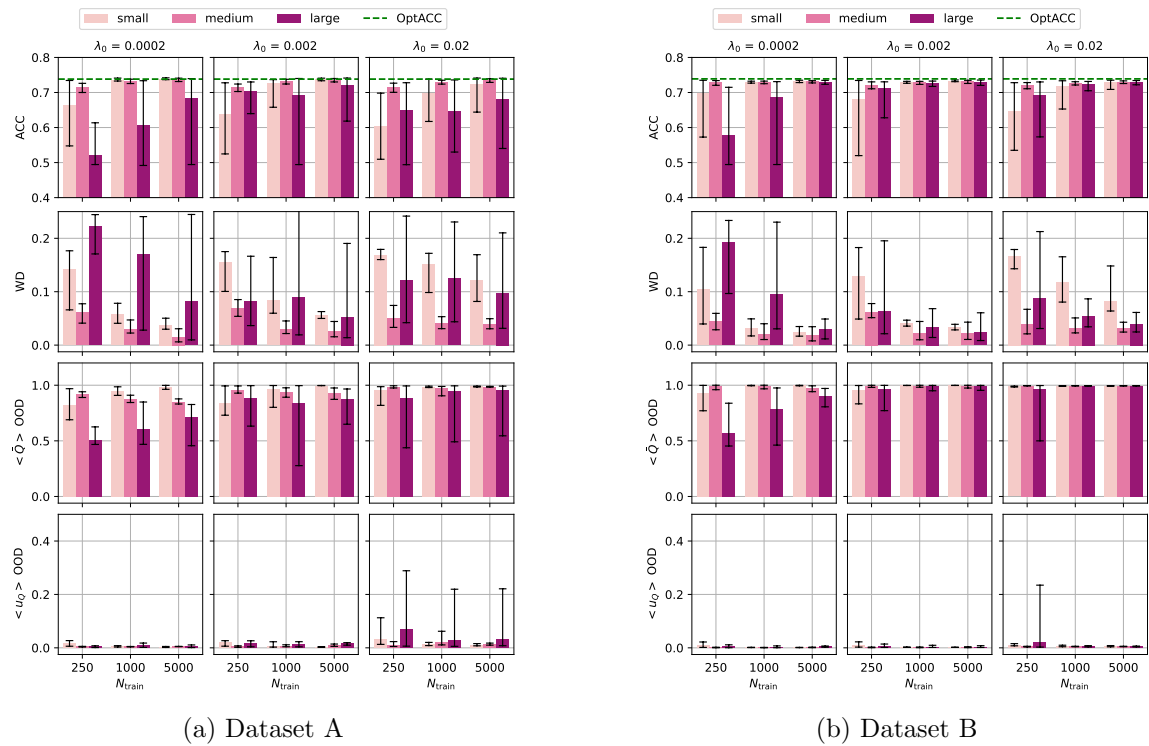


Figure 9: Results for different hyperparameter settings for evidential deep learning (EDL). Same as for Figure 7 except all the models are trained with learning rate 0.0001 and the columns show results for different values of the annealing coefficient  $\alpha$ .

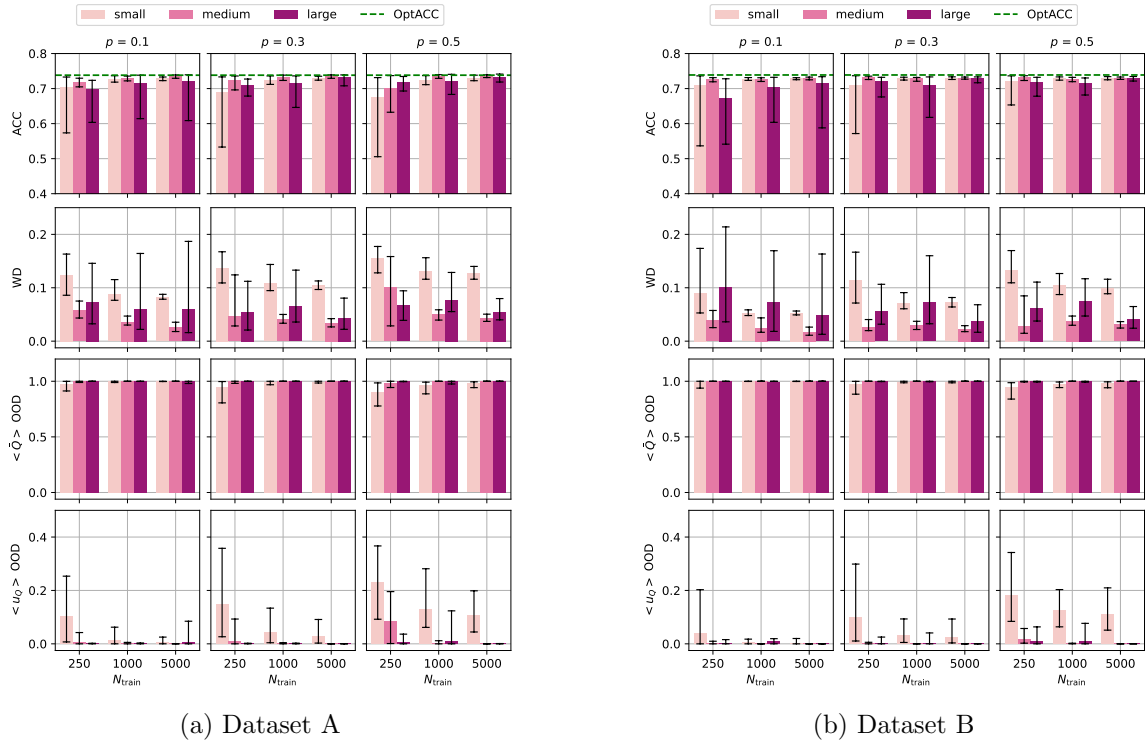


Figure 10: Results for different hyperparameter settings for neural network with Monte Carlo dropout. Same as for Figure 7 except all the models are trained with learning rate 0.001 and the columns show results for different values of the drop out rate  $p$ .

bias weight for CL (0.1, 0.2, 0.5), the annealing coefficient for EDL (0.0002/200, 0.0002/200, 0.02/200) and the drop out rate for MCD (0.1, 0.3, 0.5). For the ensembles, one ensemble with 20 networks was trained for each of the 81 different combinations of hyperparameters, while for the single network EDL and MCD algorithms 20 separate networks were trained for each combination. Weight decay was found to not have any major influence on our results, so for the study, weight decay was set to 0.01 for all algorithms. The accuracy and Wasserstein distance (WD) of the validation set, the average OOD estimated class probability and the average OOD uncertainty was calculated and are presented in Figures 7-10 as bar plots with error bars indicating the 2.5-97.5 percentiles. The  $x$ -axis of the plots show the results for different number of training points, while the color of the bar indicates the network size. The accuracy is a good measure of whether the network is properly trained. For dataset A, the optimal accuracy is 73.82% and for dataset B the optimal accuracy is 73.88%. Based on the results, any networks with less than 70% accuracy even with just 250 data points should be considered very poorly fitted. The WD is a measure of calibration, and for the validation set it should not be strongly influenced by any bias in the tails of the distribution. It is expected to go down with increasing number of training data, and hyperparameter settings which do not give results that follow this may be poor choices. The OOD estimated probability and uncertainty is also shown to see if the choice of hyperparameter would influence the results of the study. Some hyperparameter combinations do produce high uncertainties and more conservative estimated class probabilities, seemingly in conflict with our study results, but these tend to have lower accuracy scores and higher WD scores. The rest of the OOD results confirm our conclusion that NN-based estimated probabilities and uncertainties approach extreme probabilities and zero uncertainty.

Learning rate had a significant effect on results, which can be seen in Figure 7 where the results of varying learning rate and network size as well as the number of training points for the NNE algorithm is presented. Small networks need a larger learning rate, while larger networks need a smaller learning rate. For the study the medium size neural network with 3 hidden layers with 200 nodes each and a learning rate for 0.001 for all deep learning algorithms was used.

The results of varying the bias weight of the CL algorithm are presented in Figure 8. Setting the bias weight to 0.1 produced the lowest WD-scores, so this setting was used in the study. Some hyperparameter settings produce high OOD uncertainties sporadically, but these are highly variable and so could not be used as a robust anomaly detection method.

The EDL algorithm performs best across network size for annealing coefficient  $\alpha = 0.002$ . But for the ideal medium network size, it is unimportant. Larger and smaller networks show high variability in accuracy and mean WD. For dataset A, the mean estimated probability for OOD data is close to 1, but not always equal to 1. For dataset B, the estimated OOD probabilities are more extreme. Despite this, the OOD uncertainty is in most cases close to 0, even for several poorly trained networks.

For the MCD algorithm, the drop out rate does not seem to affect results much at all except for the smallest networks which also performed worse, as shown in Figure 10. In those cases, a higher drop out rate led to lower accuracies and higher WD-scores. In the study we have used a drop out rate of 0.3. Some hyperparameter settings, mainly those with small networks produce high OOD uncertainties sporadically, but these are also the ones that perform the worst on the validation set.

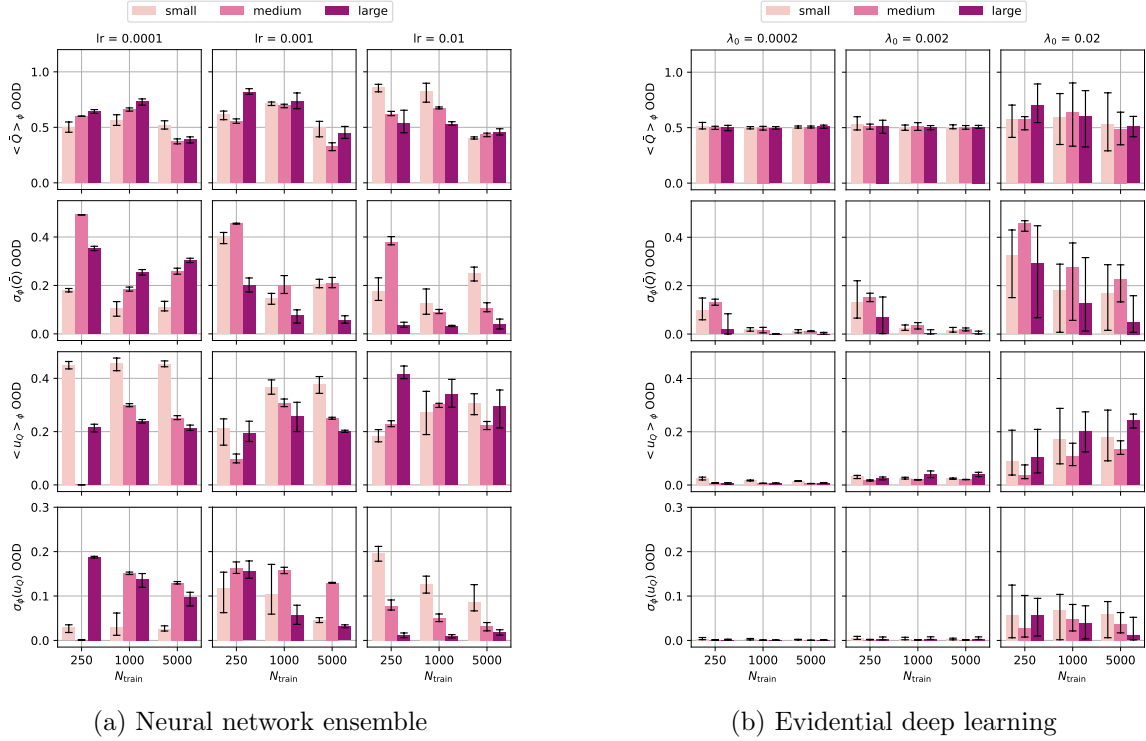


Figure 11: Results for different hyperparameter settings for neural network ensemble and evidential deep learning. The columns contain the results for learning rates 0.0001, 0.001 and 0.01. The color of the bars indicates the size and depth of the hidden layers of the network. Small, medium and large has 1, 3, and 8 hidden layers with 20, 200 and 2000 nodes respectively. The first and second rows of plots shows the mean and standard deviation of the estimated class probability for out-of-distribution test points. The bottom two rows of plots shows the mean and standard deviation of the estimated uncertainty for out-of-distribution test points. The error bars indicate the 2.5-97.5 percentiles.

In summary, the grid search corroborates our main findings and provide interesting information on the effect of the choice of different indirect priors through the hyperparameter settings.

### Appendix C. Identically distributed classes

As an additional test we created a dataset with two statistically identical classes by using the parameters of class 2 in dataset A when generating data for both classes. We ran the same hyperparameter grid search for all deep learning models. The results for NNE and EDL are presented in Figure 11. NNE, CL and MCD all produced class probability estimates which varied greatly both across hyperparameter values and as a function of polar angle. Evidential deep learning stood out as the only algorithm, which (for small enough  $\lambda_0$ ) produced estimated probabilities of 0.5. Interestingly, the uncertainty was still close to zero. The GP and DPMM algorithms struggled with this dataset, especially for large

numbers of data points so we could only evaluate performance on 2000 or less training data points. The GP hyperparameter optimization produced an output variance, which quickly approached zero as more data was added, leading to close to zero uncertainty everywhere, while the estimated probability stayed close to 0.5. For in distribution data, the DPMM gave probability estimates which were pretty noisy, as expected, but fluctuate around 0.5. Estimates for OOD data were approximately 0.5 and uncertainties were close to  $0.5/\sqrt{3}$ , in agreement with the chosen prior.

## Appendix D. 2D distributions

Figure 12 shows the spatial distribution of probability estimates, difference between the estimated distributions and the LRFD and the estimated uncertainties. These visualizations nicely illustrate the impact of the inherent spatial structures of the different models. The plain ReLU neural network models like NNE and EDL produce distributions with linear structure. MCD blurs the linear structure, creating a smoother distribution. GP with RBF kernel produces relatively smooth distributions with local radial symmetry. The specific DPMM kernels used in this study are axes-parallel bivariate Gaussians, which give the distinct grid-like structure seen in the plots. These results highlight the importance of choosing appropriate model architecture (or transforming the data to fit the model), even when the modeling tools are in theory very flexible.

## References

Moloud Abdar, Farhad Pourpanah, Sadiq Hussain, Dana Rezazadegan, Li Liu, Mohammad Ghavamzadeh, Paul Fieguth, Xiaochun Cao, Abbas Khosravi, U. Rajendra Acharya, Vladimir Makarenkov, and Saeid Nahavandi. A review of uncertainty quantification in deep learning: Techniques, applications and challenges. *Information Fusion*, 76:243–297, 2021. doi: <https://doi.org/10.1016/j.inffus.2021.05.008>.

Jose M. Bernardo and Adrian F. M. Smith. *Bayesian Theory*. Wiley series in probability and statistics. John Wiley & Sons Ltd., Chichester, 2000.

David Blei, Alp Kucukelbir, and Jon McAuliffe. Variational inference: A review for statisticians. *Journal of the American Statistical Association*, 112, 01 2016. doi: 10.1080/01621459.2017.1285773.

Zdravko I. Botev, Dirk P. Kroese, Reuven Y. Rubinstein, and Pierre L’Ecuyer. Chapter 3 - the cross-entropy method for optimization. In C.R. Rao and Venu Govindaraju, editors, *Handbook of Statistics*, volume 31 of *Handbook of Statistics*, pages 35–59. Elsevier, 2013. doi: 10.1016/B978-0-444-53859-8.00003-5.

Leo Breiman. Statistical modeling: The two cultures. *Statistical Science*, 16(3):199–215, 2001.

David B. Dunson and Abhishek Bhattacharya. Nonparametric bayes regression and classification through mixtures of product kernels. In *Bayesian Statistics 9*. Oxford University Press, 10 2011. doi: 10.1093/acprof:oso/9780199694587.003.0005.

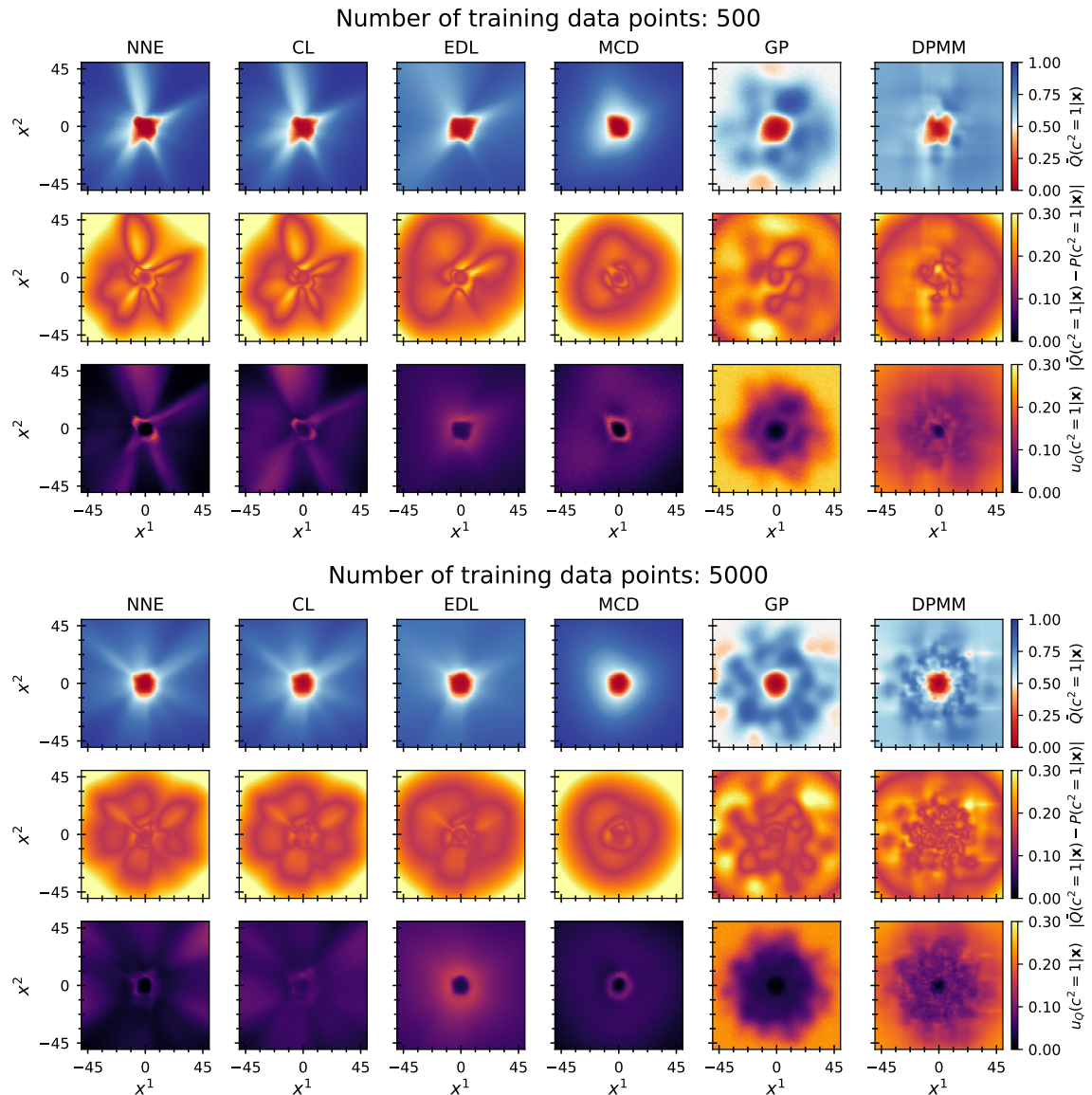


Figure 12: Estimated probabilities (top row), the absolute difference between the LRFD and the estimated probabilities (middle row) and uncertainties (bottom row) for  $N_{\text{train}} = 500$  and  $N_{\text{train}} = 5000$  (bottom) for the different algorithms in the study for dataset A.

David Duvenaud, Dougal Maclaurin, and Ryan Adams. Early stopping as nonparametric variational inference. In *Proceedings of the 19th International Conference on Artificial Intelligence and Statistics*, volume 51, pages 1070–1077. PMLR, 5 2016.

Jianqing Fan, Fang Han, and Han Liu. Challenges of big data analysis. *National Science Review*, 1(2):293–314, 02 2014. doi: 10.1093/nsr/nwt032.

Mohammed Fellaji, Frédéric Pennerath, Brieuc Conan-Guez, and Miguel Couceiro. On the calibration of epistemic uncertainty: Principles, paradoxes and conflictual loss. In *Machine Learning and Knowledge Discovery in Databases. Research Track*, page 160–176. Springer Nature Switzerland, 7 2024.

Yarin Gal and Zoubin Ghahramani. Dropout as a bayesian approximation: Representing model uncertainty in deep learning. In *Proceedings of The 33rd International Conference on Machine Learning*, volume 48, pages 1050–1059. PMLR, 6 2016.

Lei Gong and James M. Flegal. A practical sequential stopping rule for high-dimensional markov chain monte carlo. *Journal of Computational and Graphical Statistics*, 25:684–700, 7 2016. ISSN 15372715. doi: 10.1080/10618600.2015.1044092.

Chuan Guo, Geoff Pleiss, Yu Sun, and Kilian Q. Weinberger. On calibration of modern neural networks. In *Proceedings of the 34th International Conference on Machine Learning*, volume 70, pages 1321–1330. PMLR, 8 2017.

Dilan Görür and Carl Edward Rasmussen. Dirichlet process gaussian mixture models: Choice of the base distribution. *Journal of Computer Science and Technology*, 25:615–626, 2010. doi: 10.1007/s11390-010-1051-1.

Fengxiang He and Dacheng Tao. Recent advances in deep learning theory. *arXiv preprint arXiv:2012.10931*, 2020.

Matthias Hein, Maksym Andriushchenko, and Julian Bitterwolf. Why relu networks yield high-confidence predictions far away from the training data and how to mitigate the problem. In *2019 IEEE/CVF Conference on Computer Vision and Pattern Recognition (CVPR)*, pages 41–50, 2019. doi: 10.1109/CVPR.2019.00013.

Eyke Hüllermeier and Willem Waegeman. Aleatoric and epistemic uncertainty in machine learning: an introduction to concepts and methods. *Machine Learning*, 110:457–506, 3 2021. doi: 10.1007/s10994-021-05946-3.

Hemant Ishwaran and Mahmoud Zarepour. Dirichlet prior sieves in finite normal mixtures. *Statistica Sinica*, 12(3):941–963, 2002.

E. T. Jaynes. *Probability theory: The logic of science*. Cambridge University Press, Cambridge, 2003. doi: 10.1017/CBO9780511790423.

Michael Jordan, Zoubin Ghahramani, Tommi Jaakkola, and Lawrence Saul. An introduction to variational methods for graphical models. *Machine Learning*, 37:183–233, 11 1999. doi: 10.1023/A%1007665907178.

Diederik P. Kingma and Jimmy Ba. Adam: A method for stochastic optimization. In *3rd International Conference on Learning Representations*, 5 2015.

Yuelin Li, Elizabeth Schofield, and Mithat Gönen. A tutorial on dirichlet process mixture modeling. *Journal of Mathematical Psychology*, 91:128–144, 2019. doi: 10.1016/j.jmp.2019.04.004.

Yehao Liu, Matteo Pagliardini, Tatjana Chavdarova, and Sebastian U Stich. The peril of popular deep learning uncertainty estimation methods. In *Bayesian Deep Learning workshop, NeurIPS 2021*, 12 2021. doi: 10.48550/arXiv.2112.05000. URL <https://github.com/epfml/uncertainty-estimation>.

David J. C. MacKay. The evidence framework applied to classification networks. *Neural Computation*, 4(5):720–736, 1992. doi: 10.1162/neco.1992.4.5.720.

David JC MacKay. Developments in probabilistic modelling with neural networks—ensemble learning. In *Neural Networks: Artificial Intelligence and Industrial Applications: Proceedings of the Third Annual SNN Symposium on Neural Networks*, pages 191–198. Springer, 9 1995.

Stephan Mandt, Matthew D Hoffman, and David M Blei. Stochastic gradient descent as approximate bayesian inference. *Journal of Machine Learning Research*, 18(134):1–35, 2017.

Fabrizio Maturo, Salvador Cruz Rambaud, and Viviana Ventre. Advances in statistical learning from high-dimensional data. *Quality and Quantity*, 59:1933, 6 2025. ISSN 15737845. doi: 10.1007/s11135-025-02242-3.

Matthias Minderer, Josip Djolonga, Rob Romijnders, Frances Hubis, Xiaohua Zhai, Neil Houlsby, Dustin Tran, and Mario Lucic. Revisiting the calibration of modern neural networks. In *Advances in Neural Information Processing Systems*, volume 34, pages 15682–15694. Curran Associates, Inc., 2021.

Mahdi Pakdaman Naeini, Gregory F. Cooper, and Milos Hauskrecht. Obtaining well calibrated probabilities using bayesian binning. In *Proceedings of the Twenty-Ninth AAAI Conference on Artificial Intelligence*, AAAI’15, page 2901–2907. AAAI Press, 2 2015.

Alexandru Niculescu-Mizil and Rich Caruana. Predicting good probabilities with supervised learning. In *ICML 2005 - Proceedings of the 22nd International Conference on Machine Learning*, pages 625–632, 01 2005. doi: 10.1145/1102351.1102430.

Jeremy Nixon, Michael W Dusenberry, Linchuan Zhang, Ghassen Jerfel, and Dustin Tran. Measuring calibration in deep learning. In *CVPR workshops*, volume 2, 2019.

F. Pedregosa, G. Varoquaux, A. Gramfort, V. Michel, B. Thirion, O. Grisel, M. Blondel, P. Prettenhofer, R. Weiss, V. Dubourg, J. Vanderplas, A. Passos, D. Cournapeau, M. Brucher, M. Perrot, and E. Duchesnay. Scikit-learn: Machine learning in Python. *Journal of Machine Learning Research*, 12:2825–2830, 2011.

Alexandre Perez-Lebel, Marine Le Morvan, and Gaël Varoquaux. Beyond calibration: estimating the grouping loss of modern neural networks. In *The Eleventh International Conference on Learning Representations*, pages 10784–10831, 4 2023. doi: 10.48550/arXiv.2210.16315.

Pascal Pernot. Calibration in machine learning uncertainty quantification: Beyond consistency to target adaptivity. *APL Machine Learning*, 1(4):046121, 12 2023. doi: 10.1063/5.0174943.

Piero Giovanni Luca Porta-Mana. Foundations of inference under symmetry: An algorithm for non-parametric density inference, 2025. URL [https://github.com/pglpm/inferno/raw/main/development/manual/optimal\\_predictor\\_machine.pdf](https://github.com/pglpm/inferno/raw/main/development/manual/optimal_predictor_machine.pdf). Accessed: 26-06-2025.

Piero Giovanni Luca Porta-Mana, Håkon Mydland, Maksim Ohrvill, Aurora grefsrud, and Simen Hesthamar Hauge. Inferno v0.2.1, 2024. URL <https://github.com/pglpm/inferno>.

Aaditya Ramdas, Nicolás García Trillos, and Marco Cuturi. On wasserstein two-sample testing and related families of nonparametric tests. *Entropy*, 19(2), 2017. doi: 10.3390/e19020047.

Carl Edward. Rasmussen and Christopher K. I.. Williams. *Gaussian processes for machine learning*. MIT Press, 2006.

Alexander Reutlinger, Dominik Hangleiter, and Stephan Hartmann. Understanding (with) toy models. *The British Journal for the Philosophy of Science*, 69:1069–1099, 07 2018. doi: 10.1093/bjps/axx005.

Donald B Rubin. Bayesianly justifiable and relevant frequency calculations for the applied statistician. *The Annals of Statistics*, pages 1151–1172, 1984.

Murat Sensoy, Lance Kaplan, and Melih Kandemir. Evidential deep learning to quantify classification uncertainty. In *Advances in Neural Information Processing Systems*, volume 31, page 3179–3189, 12 2018. doi: 10.48550/arXiv.1806.01768. URL <https://github.com/dougbrion/pytorch-classification-uncertainty>.

Shubhendu Trivedi and Brian D Nord. On the need to align intent and implementation in uncertainty quantification for machine learning. *arXiv preprint arXiv:2506.03037*, 2025.

C.K.I. Williams and D. Barber. Bayesian classification with gaussian processes. *IEEE Transactions on Pattern Analysis and Machine Intelligence*, 20(12):1342–1351, 1998. doi: 10.1109/34.735807.

Mu Zhu and Arthur Y Lu. The counter-intuitive non-informative prior for the bernoulli family. *Journal of Statistics Education*, 12(2), 2004.